

Study of domain boundary polarization in (111)-cut $[\text{Pb}(\text{Mg}_{1/3}\text{Nb}_{2/3})\text{O}_3]_{0.7}(\text{PbTiO}_3)_{0.3}$ single crystal by piezoresponse force microscopy

K. S. Wong, X. Zhao, J. Y. Dai,^{a)} and C. L. Choy^{a)}

Department of Applied Physics, The Hong Kong Polytechnic University, Hung Hom, Kowloon, Hong Kong, People's Republic of China

X. Y. Zhao and H. S. Luo

State Key Laboratory of High Performance Ceramics and Superfine Microstructure, Shanghai Institute of Ceramics, Chinese Academy of Sciences, 215 Chengbei Road, Jiading, Shanghai 201800, People's Republic of China

(Received 29 May 2006; accepted 9 July 2006; published online 30 August 2006)

Ferroelectric domain structure, especially the domain boundary polarization, in as-grown and poled (111)-cut PMN-30%PT single crystal has been studied by means of out-of-plane and in-plane piezoresponse force microscopies (PFMs). It revealed that the as-grown sample exhibits speckle-shaped microdomains, and the domain number distribution decreases exponentially as the domain size increases which can be described by the random field Ising model; in contrast, the poled sample shows stripe-shaped domains. Capacitive force-free PFM revealed a detailed domain boundary characteristic with net in-plane polarization. The presence of the in-plane polarization at the domain boundary also suggests the existence of orthorhombic phase in the rhombohedral matrix. © 2006 American Institute of Physics. [DOI: 10.1063/1.2339038]

Recently, the study of relaxor ferroelectric single crystal, $[\text{Pb}(\text{Mg}_{1/3}\text{Nb}_{2/3})\text{O}_3]_{1-x}(\text{PbTiO}_3)_x$ (PMN-*x*PT), is attracting a great deal of attention because of their high piezoelectric coefficient ($d_{33} \sim 2000$ pC/N) and electromechanical coupling factor ($k_{33} \sim 92\%$),^{1,2} and large potential in application of novel devices such as electromechanical sensors, ultrasound transducers, and actuators. PMN-*x*PT has the complex perovskite structure with an ABO_3 -type unit cell and exhibits a diffuse phase transition in a wide temperature range with a frequency-dependent dielectric maximum at temperature T_m which represents the transition temperature from ferroelectric to paraelectric phase.^{3,4} In the morphotropic phase boundary in the range of $x=28\% - 36\%$ of PT,⁵ PMN-*x*PT single crystal has a complex phase diagram with rhombohedral (*R*), tetragonal (*T*), orthorhombic (*O*), and monoclinic (*M*) phases.^{2,6}

The domain structure and phase transition in ferroelectric material have been investigated commonly by means of polarizing optical microscopy.⁷⁻¹⁰ However, the optical microscopy has a drawback of limited resolution. Therefore, more researchers are studying the ferroelectric domains by means of piezoresponse force microscopy (PFM),^{1,11-15} which is able to reveal the domain structure with high spatial resolution and sensitivity to local polarization. In addition, for three-dimensional polarization analyses in ferroelectric materials, in-plane polarization (IPP) and out-of-plane polarization (OPP) PFM imaging techniques have been implemented simultaneously. For example, Kim *et al.*¹¹ have reported their study of IPP and OPP of BaTiO_3 thin films by means of PFM. Many investigations of ferroelectric domain structure through PFM imaging have been carried out. However, the domain boundary structure study in the PMN-*x*PT single crystal by PFM is rare. In this letter, we report the

investigation result of domain boundary structure in the (111)-cut PMN-30%PT single crystals by means of PFM with IPP and OPP imagings.

The PMN-30%PT single crystal was grown by using the modified Bridgman technique.¹⁶ The (111)-cut PMN-30%PT samples were mechanically polished to optical quality with the thickness of about 15 μm in order to minimize superposition of domains. In order to investigate the domain structure, Cr/Au was coated on the bottom of samples as electrode, and one sample was coated with a top electrode and poled along the $\langle 111 \rangle$ direction by an electric field of 10 kV/cm at 110 °C for 20 min and of 5 kV/cm in the cooling process. The domain images were obtained by piezoresponse force microscope (Nanoscope IV, Digital Instruments) utilizing a conductive tip coated with Cr/Pt. For the PFM imaging, a modulating voltage of 6 V (peak to peak) with 11 kHz was applied to the bottom electrode of sample, while the tip was electrically grounded. The IPP and OPP images were obtained by collecting the piezoelectric response signal demodulated by two lock-in amplifiers.

It has been reported that a skin effect presents in the relaxor ferroelectrics of PZN-*x*PT and PMN-*x*PT systems in which the skin layer thickness is around a few micrometers or above.¹⁷⁻¹⁹ In considering this, we have annealed the samples at 170 °C ($>T_m$) for 30 min before imaging and poling in order to minimize the skin effect and also release the stress due to polishing. In addition, in PFM imaging, the piezoresponse is from the whole sample thickness to the applied electric field. Therefore, unless the sample is extremely thin, for example, less than 10 μm , the PFM images are believed mainly from bulk effect.

The OPP piezoresponse amplitude and phase images of the as-grown (111)-cut PMN-30%PT single crystal without capacitive force are shown in Fig. 1. The speckle-shaped domains with a varying size can be observed, and it is apparent that there are a larger number of small nanodomains

^{a)}Electronic mail: apdaijy@inet.polyu.edu.hk

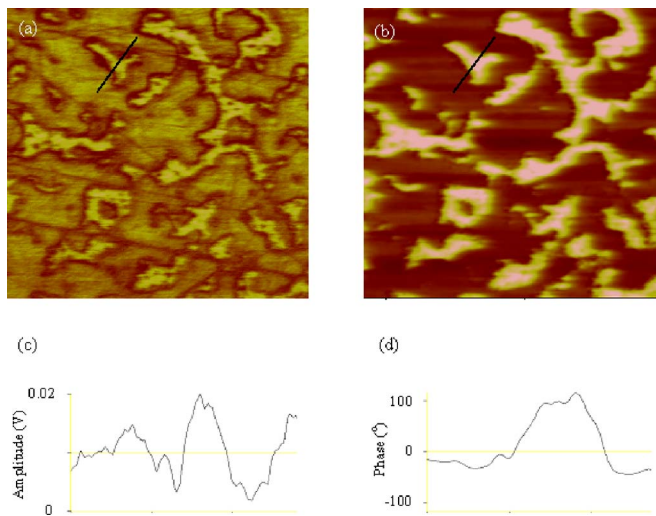


FIG. 1. (Color online) Piezoresponse OPP (a) amplitude and (b) phase images of the as-grown (111)-cut PMN-30%PT single crystal with a scan size of $5 \mu\text{m}$. [(c) and (d)] The cross-sectional analysis of the black line in (a) and (b), respectively.

(about a few tens of nanometers) embedded in the micro-sized domains which can be attributed to the local random field induced polar nanosized regions (PNRs) in the PMN- x PT single crystal.¹² Based on the results of Shvartsman and Kholkin and Zhao *et al.*, in PMN-20%PT and PMN-25%PT single crystals, the two-dimensional random field Ising model (RFIM) well described the relaxor ferroelectric properties of their samples,^{12,13} and the domain pattern under strong random field predicted by the RFIM is similar to our piezoresponse phase image, as shown in Fig. 1(b).²⁰

In the PFM image, the domain size distribution of relaxor ferroelectrics follows a power law with an exponential cutoff, i.e.,

$$N_d(S_d) \sim S_d^{-\delta} \exp\left(-\frac{S_d}{S_0}\right), \quad (1)$$

where N_d is the number of domains with size of S_d , and S_0 is the upper cutoff of domain size. The relationship between the number of domains and the domain size in the as-grown (111)-cut PMN-30%PT single crystal is shown in Fig. 2,

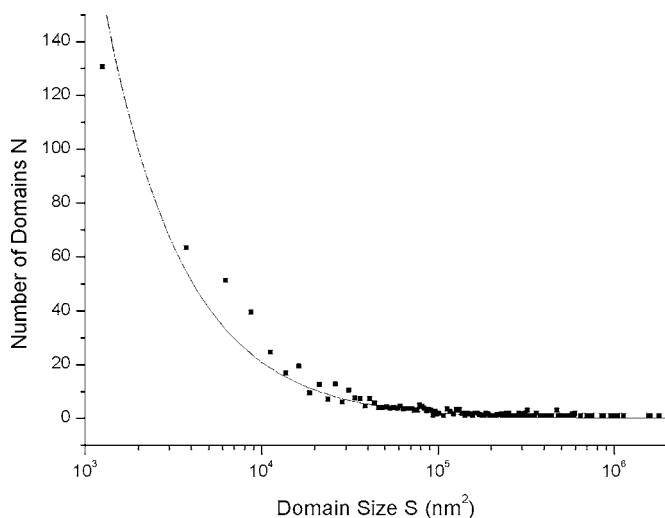


FIG. 2. Domain size distribution of the as-grown (111)-cut PMN-30%PT single crystal. The solid line represents the fit to Eq. (1).

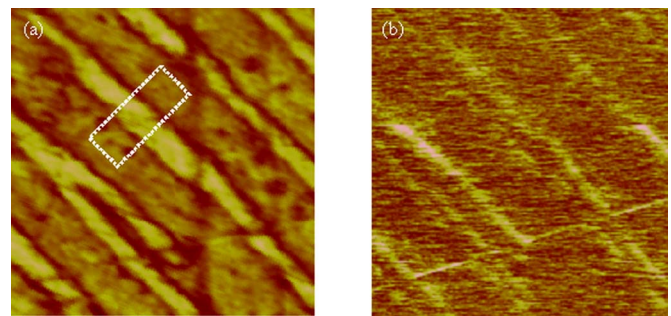


FIG. 3. (Color online) Piezoresponse (a) OPP amplitude image without capacitive force effect of the poled (111)-cut PMN-30%PT single crystal with a scan size of $7 \mu\text{m}$. (b) The IPP amplitude image corresponding to (a).

where the data points were collected by the analysis function of the DI software (Digital Instruments). The domain size distribution fits well with Eq. (1) with the value of exponent $\delta=0.96$ and $S_0=7.4 \times 10^5 \text{ nm}^2$. This fitted value of exponent δ is less than that found in the PFM imaging analyses on the PMN-25%PT single crystal¹³ ($\delta=2.41$), suggesting that the variation of the number of nanodomains in the PMN-30%PT single crystal is smaller for higher content of PT.

It is interesting to notice that in Fig. 1(a), a very clear contrast of domain boundary with a thickness in the range of 50–100 nm can be observed. The dark contrast in the amplitude image corresponds to the regions without piezoresponse signal in the out-of-plane direction, and the bright regions possess large out-of-plane piezoresponse. While in the phase, the upward (pointing out of the paper) OPP appears dark in contrast, and regions with downward OPP appear bright, as shown in Fig. 1(b). The cross-sectional signal analyses of the black lines in Figs. 1(a) and 1(b) are shown in Figs. 1(c) and 1(d), respectively. It is worth noting that a large force constant tip was used in PFM imaging in order to increase the signal to noise ratio and the capacitive force effect has been significantly reduced. The capacitive force is the attractive force between cantilever and sample that alter the PFM image and shadow the information of domain boundary structure. Hong *et al.* investigated the capacitive force during PFM imaging and found out that it can be reduced by placing the tip near the edge of sample surface.²¹ As an alternative approach, we coated a conductive layer on the sample surface and removed a part of the coating before PFM imaging; and therefore, a clear domain boundary feature can be achieved in the PFM image, as shown in Fig. 1(a).

Figure 3 shows the OPP and IPP PFM images of the poled (111)-cut PMN-30%PT sample at room temperature where stripe domains can be observed. OPP PFM image without capacitive force effect is shown in Fig. 3(a), where the narrow (about $0.5 \mu\text{m}$) and wide ($1\text{--}2 \mu\text{m}$) bright stripes correspond to different orientation of polarizations. Without the capacitive force effect in PFM imaging, both upward and downward domains appear bright in the amplitude image, where they appear bright and dark in the phase image (not shown). It is interesting to notice that the dark contrast with the width of about 100–200 nm at the domain boundaries in Fig. 3(a), however, appears bright in the IPP image, as shown in Fig. 3(b). This indicates that the domain boundaries are with a certain thickness containing large in-plane polarization component with very little or zero out-of-plane component.

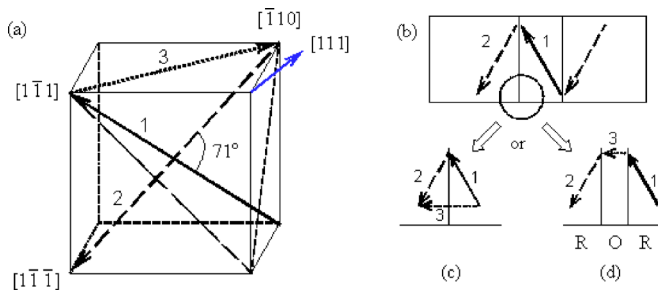


FIG. 4. (Color online) (a) Local polarizations in pseudocubic axes. (b) The schematic diagram of proposed domain configuration of the poled (111)-cut PMN-30%PT single crystal in Fig. 3(a). [(c) and (d)] Two explanations of domain structure for the observation in PFM images.

The sample was poled along the $[111]$ direction. However, due to the depolarization which is evidenced by the appearance of the striplike domain contrast, other $\langle 111 \rangle$ polarizations will present in the poled sample in order to minimize the system energy. To illustrate the domain polarization, Fig. 4(a) shows the $\langle 111 \rangle$ polarizations indicated by the solid $[1\bar{1}\bar{1}]$ and short dash $[\bar{1}\bar{1}\bar{1}]$ arrows representing the upward and downward polarizations in the cross-sectional diagram of Fig. 4(b). In our opinion, there are two possible explanations about the large in-plane polarization at the domain boundaries, as shown in Figs. 4(c) and 4(d). According to Fig. 4(c), at the domain boundaries the polarizations have been divided into OPP and IPP components. The OPP components of the $\langle 111 \rangle$ polarizations (1) and (2) cancel out each other, and their IPP components are added together to form a pure IPP polarization (3) at the domain boundaries. It is well known that the thickness of a ferroelectric domain boundary is only a few-atomic-layer thick, but our result shows a more than 100-nm-thick domain boundary layer. This may be explained by the strong IPP polarization at the domain boundary resulting in a large piezoresponse signal; and therefore the domain boundary thickness observed by the IPP PFM is larger than the real thickness.

We propose another possible explanation to the existence of an in-plane polarization layer at the domain boundary. In Figs. 4(a) and 4(d), the $\langle 110 \rangle$ in-plane polarization (3) belongs to an orthorhombic phase which presents in the rhombohedral matrix of PMN-30%PT single crystal.^{2,22} Recently, Xu *et al.*²³ have reported high-energy x-ray diffuse-scattering measurements on the relaxor $\text{Pb}(\text{Zn}_{1/3}\text{Nb}_{2/3})\text{O}_3$ (PZN) single crystal after an electric field poling along the $\langle 111 \rangle$ direction. They found the existence of polar nanosized regions with in-plane $\langle 110 \rangle$ -type polarizations in the rhombohedral matrix of PZN single crystal. Therefore, based on our proposed model, the $\langle 110 \rangle$ polarization is possibly the domain bound-

ary phase in the rhombohedral phase matrix. This may present a direct evidence to show the existence and location of the orthorhombic phase in the rhombohedral matrix of PMN-xPT single crystal at the morphotropic phase boundary.

In summary, the as-grown and poled (111)-cut PMN-30%PT single crystals have been investigated by means of piezoresponse force microscopy at room temperature, and the results revealed different domain structures. In the poled sample, the stripe-shaped domains are observed by the OPP PFM imaging, and large IPP component presents in the domain boundaries with certain thickness. Orthorhombic phase may present as the domain boundary phase in the poled (111)-cut PMN-30%PT single crystal.

This project is supported by the Hong Kong RGC grant (No. B-Q772). One of the authors, K.S.W., is grateful to F. G. Shin for encouraging discussion.

- ¹X. Zhao, J. Y. Dai, J. Wang, H. L. W. Chan, C. L. Choy, X. M. Wan, and H. S. Luo, *J. Appl. Phys.* **97**, 094107 (2005).
- ²Y. P. Guo, H. S. Luo, K. P. Chen, H. Q. Xu, X. W. Zhang, and Z. W. Yin, *J. Appl. Phys.* **92**, 6134 (2002).
- ³X. Y. Zhao, J. Wang, H. L. W. Chan, C. L. Choy, and H. S. Luo, *Appl. Phys. A: Mater. Sci. Process.* **80**, 653 (2005).
- ⁴X. Y. Zhao, Ph.D. thesis, Chinese Academy of Sciences, 2004.
- ⁵C. S. Tu, C. L. Tsai, J. S. Chen, and V. H. Schmidt, *Phys. Rev. B* **65**, 104113 (2002).
- ⁶B. Noheda, D. E. Cox, G. Shirane, J. Gao, and Z. G. Ye, *Phys. Rev. B* **66**, 054104 (2002).
- ⁷C. S. Tu, V. H. Schmidt, I. C. Shih, and R. Chien, *Phys. Rev. B* **67**, 020102 (2003).
- ⁸C. S. Tu, I. C. Shih, V. H. Schmidt, and R. Chien, *Appl. Phys. Lett.* **83**, 1833 (2003).
- ⁹Z. G. Ye and M. Dong, *J. Appl. Phys.* **87**, 2312 (2000).
- ¹⁰R. R. Chien, V. H. Schmidt, L. W. Hung, and C. S. Tu, *J. Appl. Phys.* **97**, 114112 (2005).
- ¹¹I. D. Kim, Y. Avrahami, H. L. Tuller, Y. B. Park, M. J. Dicken, and H. A. Atwater, *Appl. Phys. Lett.* **86**, 192907 (2005).
- ¹²V. V. Shvartsman and A. L. Kholkin, *Phys. Rev. B* **69**, 014102 (2004).
- ¹³X. Zhao, J. Y. Dai, J. Wang, H. L. W. Chan, C. L. Choy, X. M. Wan, and H. S. Luo, *Phys. Rev. B* **72**, 064114 (2005).
- ¹⁴H. R. Zeng, H. F. Yu, R. Q. Chu, G. R. Li, H. S. Luo, and Q. R. Yin, *Mater. Lett.* **59**, 238 (2005).
- ¹⁵F. Bai, J. F. Li, and D. Viehland, *Appl. Phys. Lett.* **85**, 2313 (2004).
- ¹⁶H. S. Luo, G. S. Xu, H. Q. Xu, P. C. Wang, and Z. W. Yin, *Jpn. J. Appl. Phys., Part 1* **39**, 5581 (2000).
- ¹⁷B. Noheda, D. E. Cox, G. Shirane, S.-E. Park, L. E. Cross, and Z. Zhong, *Phys. Rev. Lett.* **86**, 3891 (2001).
- ¹⁸G. Xu, H. Hiraka, G. Shirane, and K. Ohwada, *Appl. Phys. Lett.* **84**, 3975 (2004).
- ¹⁹G. Xu, P. M. Gehring, C. Stock, and K. Conlon, *Phase Transitions* **79**, 135 (2006).
- ²⁰J. Esser, U. Nowak, and K. D. Usadel, *Phys. Rev. B* **55**, 5866 (1997).
- ²¹S. Hong, H. Shin, J. Woo, and K. No, *Appl. Phys. Lett.* **80**, 1453 (2002).
- ²²M. Shanthi, S. M. Chia, and L. C. Lim, *Appl. Phys. Lett.* **87**, 202902 (2005).
- ²³G. Xu, Z. Zhong, Y. Bing, Z.-G. Ye, and G. Shirane, *Nat. Mater.* **5**, 134 (2006).